

Ruckerbactin produced by *Yersinia ruckeri* YRB is a
diastereomer of the siderophore trivanchrobactin
produced by *Vibrio campbellii* DS40M4

*Emil Thomsen, Zachary L. Reitz, Parker R. Stow, Kalana Dulaney, Alison Butler**

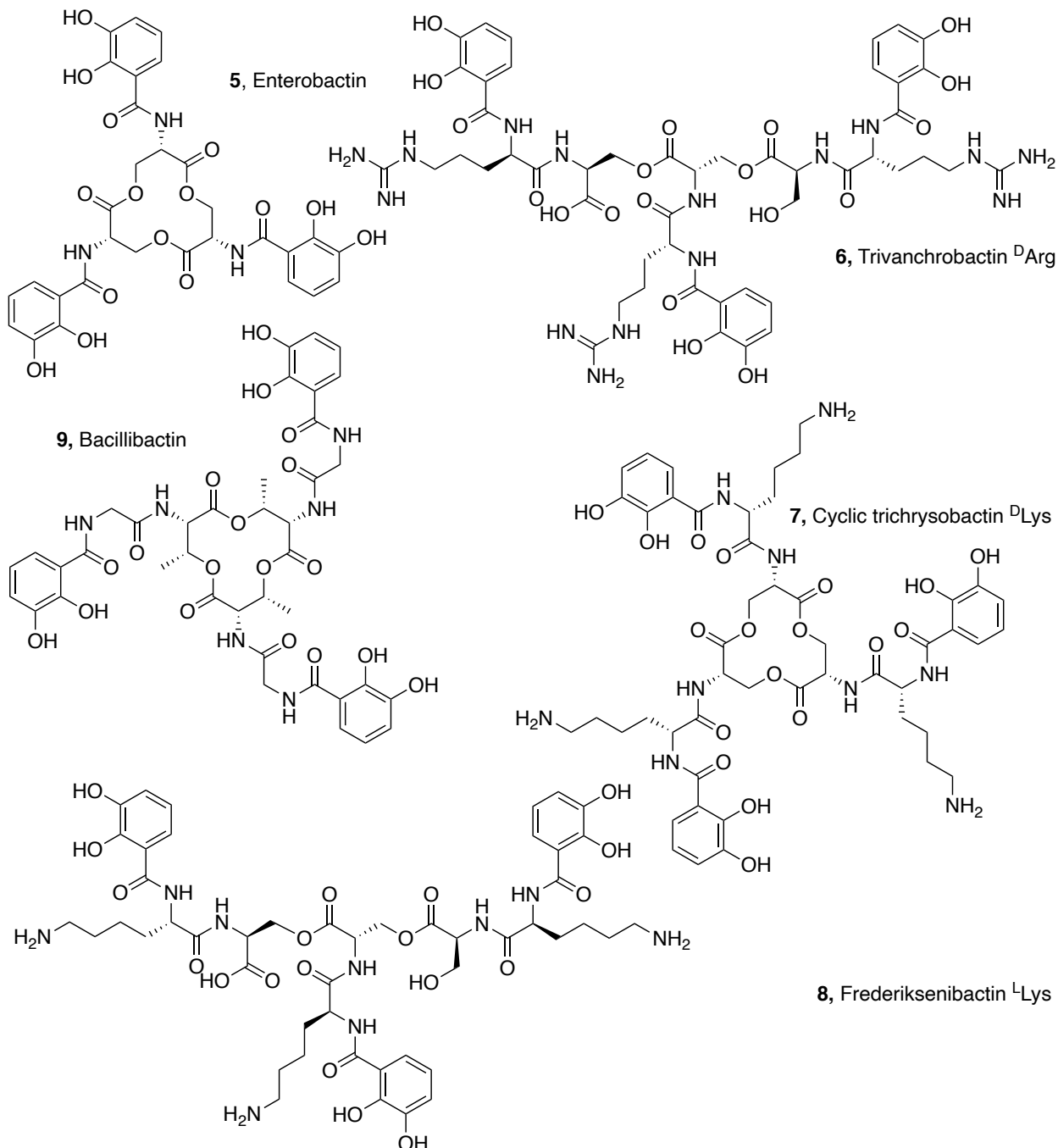
Department of Chemistry & Biochemistry, University of California, Santa Barbara, CA 93106

ABSTRACT

The Gram-negative bacterium *Yersinia ruckeri* is the causative agent for enteric red mouth disease in salmonids. The genome of *Y. ruckeri* YRB contains a biosynthetic gene cluster encoding the biosynthesis of catechol siderophores that are diastereomeric with the known vanchrobactin class of siderophores, (DHB^DArg^LSer)₍₁₋₃₎. Ruckerbactin (**1**), produced by *Y. ruckeri* YRB, was found to be the linear tris-L-serine ester comprised of L-arginine and 2,3-dihydroxybenzoic acid, (DHB^LArg^LSer)₃. The biscatechol, (DHB^LArg^LSer)₂ (**2**) and monocatechol, DHB^LArg^LSer (**3**) compounds were also isolated and characterized. The macrolactone of ruckerbactin was not detected. The presence of ^LArg in ruckerbactin makes it the diastereomer of trivanchrobactin with ^DArg. The circular dichroism spectra of Fe(III)-ruckerbactin and Fe(III)-trivanchrobactin reveal the opposite enantiomeric configurations at the Fe(III) sites. Fe(III)-ruckerbactin adopts the Δ configuration and Fe(III)-trivanchrobactin adopts the Λ configuration. *Y. ruckeri* YRB was also found to produce the antimicrobial agent holomycin (**4**).

Introduction

Many bacteria produce siderophores, which are secondary metabolites that facilitate the acquisition of iron required for growth. Siderophores are known for their substantial Fe(III) affinity constants which enable solubilization of colloidal ferric oxides or sequestration of Fe(III) from iron proteins. The archetypic siderophore enterobactin (**5**), produced by many enteric and pathogenic microbes, is a triscatecholamide siderophore framed on a cyclic macrolactone backbone of ^LSer in which each Ser amine is appended by the catechol 2,3-dihydroxybenzoate (DHB). Nature has capitalized on the oligo-^LSer core as observed for example in trivanchrobactin (**6**),¹ cyclic trichrysobactin (**7**),² frederiksenibactin (**8**),³ and in the oligo ^LThr core as observed for example in bacillibactin (**9**).⁴ With the exception of enterobactin, the other serine-based tris catechol siderophores are distinguished by the presence of an amino acid spacer between ^LSer and 2,3-DHBA. Trivanchrobactin, cyclic trichrysobactin and turnerbactin (not shown) each contain a cationic amino acid inserted between the oligoester ^LSer scaffold and 2,3-DHB – that is, ^DArg, ^DLys and L-ornithine (^LOrn), respectively.^{1, 2, 5} Similarly bacillibactin and griseobactin (not shown) contain Gly and ^LArg spacers, respectively, between the oligo ester of ^LThr and 2,3-DHB.^{6, 7}



The Gram-negative bacterium *Yersinia ruckeri* is the causative agent for enteric red mouth disease in salmonids.⁸ Numerous strains of *Y. ruckeri* have been found to produce a catechol siderophore, called ruckerbactin.⁹ However, this catechol siderophore was unable to support the growth of *Salmonella typhimurium* deficient in enterobactin biosynthesis, suggesting it differs substantially from enterobactin.¹⁰ Knocking out the *rucC* gene, the homolog of *entC*, which

encodes the first committed enzyme in the biosynthesis of 2,3-DHBA, leads to a 100 fold increase in the 50% lethal dose tests.⁹ The *rucC* knockout results emphasize the importance of ruckerbactin in colonization of its host. However, while some of the biological effects of ruckerbactin are known, including which genes are upregulated under iron limiting conditions,¹¹ the structure of ruckerbactin has evaded elucidation until now.

Analysis of the ruckerbactin gene cluster of *Yersinia ruckeri* YRB led to a predicted structure of ruckerbactin as a diastereomer of vanchrobactin, DHB^DArg^LSer,¹ or trivanchrobactin (**6**), (DHB^DArg^LSer)₃.¹ We report herein the structural characterization of ruckerbactin, along with the stereochemistry of the Fe(III)-ruckerbactin complex in comparison to its diastereomer Fe(III)-trivanchrobactin. In addition to ruckerbactin, we characterized of two smaller compounds related to ruckerbactin, as well as, the antimicrobial agent holomycin.

Results and Discussion

Through bioinformatics and genome mining approaches applied to microbial genome sequences, we identified a distinct BGC in *Y. ruckeri* YRB which is related to the *vab* locus encoding biosynthesis of trivanchrobactin in *Vibrio campbellii* DS40M4. This gene cluster was previously identified and was determined to encode for the biosynthesis and transport of a catechol siderophore named *ruckerbactin*; however, no structural characterization of this compound was performed.⁹ The *ruc* locus contains homologs of *entABCE* encoding the biosynthesis and activation of 2,3-DHBA, and *rucF* encoding a non-ribosomal peptide synthetase (NRPS) (Figure 1A). The RucF adenylation domains are predicted to have the same selectivity as VabF of vanchrobactin biosynthesis, Arg and Ser (Figure 1B). The distinction occurs within the first module of the ruckerbactin NRPS RucF, which lacks the epimerization domain of VabF responsible for converting ^LArg to ^DArg in vanchrobactin and trivanchrobactin.

Therefore, *Y. ruckeri* YRB is predicted to produce a siderophore composed of 1-3 units of (DHB^LArg^LSer), thus placing it in a diastereomeric relationship to vanchrobactin, divanchrobactin and trivanchrobactin.

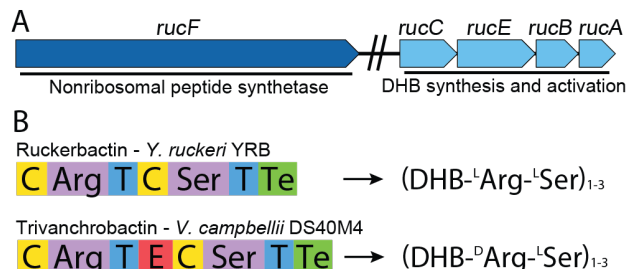


Figure 1. Biosynthetic gene clusters of ruckerbactin (*Y. ruckeri* YRB) and trivanchrobactin (*V. campbellii* DS40M4)

To isolate the ruckerbactin siderophore, *Y. ruckeri* YRB was grown in a low-iron minimal medium. The methanolic eluent from the solid-phase extraction of the culture supernatant yielded the siderophore-containing crude extract. Analytical HPLC of this methanolic extract revealed the presence of four peaks (Figure S1). The UV absorbance of peaks 1-3 at $\lambda_{\text{max}} \sim 250$ nm and ~ 310 nm is consistent with the presence of catechol, as was also observed for vanchrobactin.¹ High resolution electrospray ionization mass spectrometry (HRESI-MS) established the molecular ion of ruckerbactin (**1**) $[\text{M}+\text{H}]^+$ as *m/z* 1156.4657 (Figure S2). The HRESI-MS of compounds **2** and **3** revealed molecular ions $[\text{M}+\text{H}]^+$ at *m/z* 777.3178 and *m/z* 398.1675 (Figure S2). These ions are consistent with the molecular composition of ruckerbactin **1** as $\text{C}_{48}\text{H}_{65}\text{N}_{15}\text{O}_{19}$. Compound **2** is consistent with $\text{C}_{32}\text{H}_{44}\text{N}_{10}\text{O}_{13}$ and compound **3** is consistent with $\text{C}_{16}\text{H}_{23}\text{N}_5\text{O}_7$. ESI tandem mass spectrometry (ESI-MS/MS) of peaks **1-3** gave rise to several fragments in agreement with a DHB-Arg-Ser core structure, as was also observed in the siderophore vanchrobactin.¹ Loss of the catechol was identified for compound **1-3** by fragments with *m/z* 137.07 (*b*₁) and 154.05(*c*₁) (Figure 3 and Figures S3-S5). The loss of the catechol also

gave rise to the Arg-Ser fragment m/z 262.15 (y_1^+) for compound **3**; m/z 321.15 (y_1^{2+}) for compound **2**, and m/z 340.80 (y_1^{3+}) for ruckerbactin (Figures S3-S5). For compound **3**, fragmentation between Ser and Arg produced fragments with m/z 293.12 (b_2) and m/z 311.13 (c_2) (Figure S3). For compound **2** similar fragmentation gave the ions m/z 293.12 (b_2), m/z 311.13 (c_2) and m/z 485.2 (y_2) (Figure S4). Finally, for ruckerbactin fragmentation between Arg and Ser formed fragments with m/z 311.13 (c_2), m/z 293.12 (b_2) and m/z 432.68 (y_2^{2+}) (Figure 3). Signals originating from the cleavage of the serine ester(s) were identified in ruckerbactin as m/z 380.17, m/z 398.17 and m/z 389.16, and for **2** as m/z 398.17 and m/z 380.16. Fragments characteristic of Arg are also evident in the tandem mass spectra of **1**, **2** and **3**,¹² with the ion at m/z 175.12 and further supported by masses reflecting the loss of NH_3 , m/z 158.10; the loss of H_2O , m/z 157.11; the loss of $\text{CO}+\text{NH}_3$, m/z 130.09; and the loss of $\text{CO}+\text{NH}_3+\text{H}_2\text{O}$, m/z 112.08.

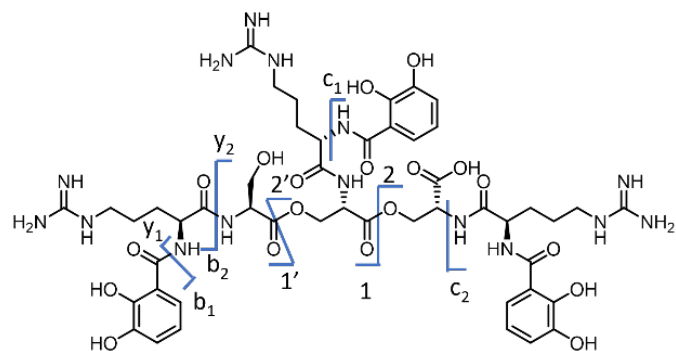
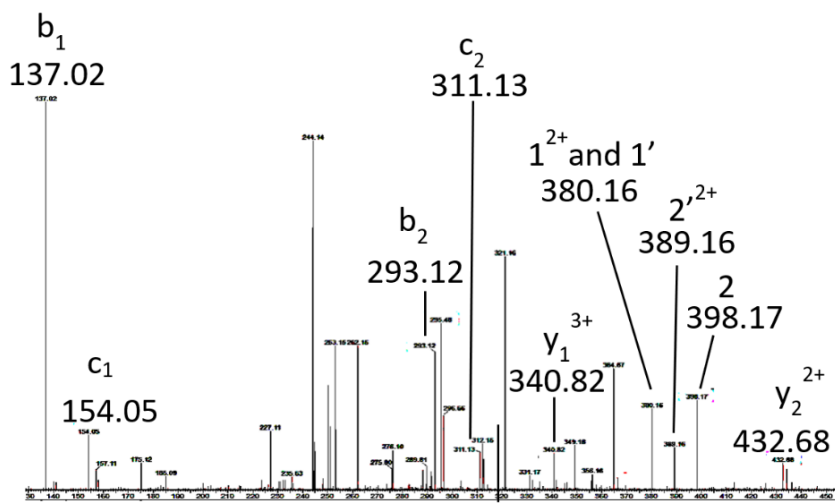
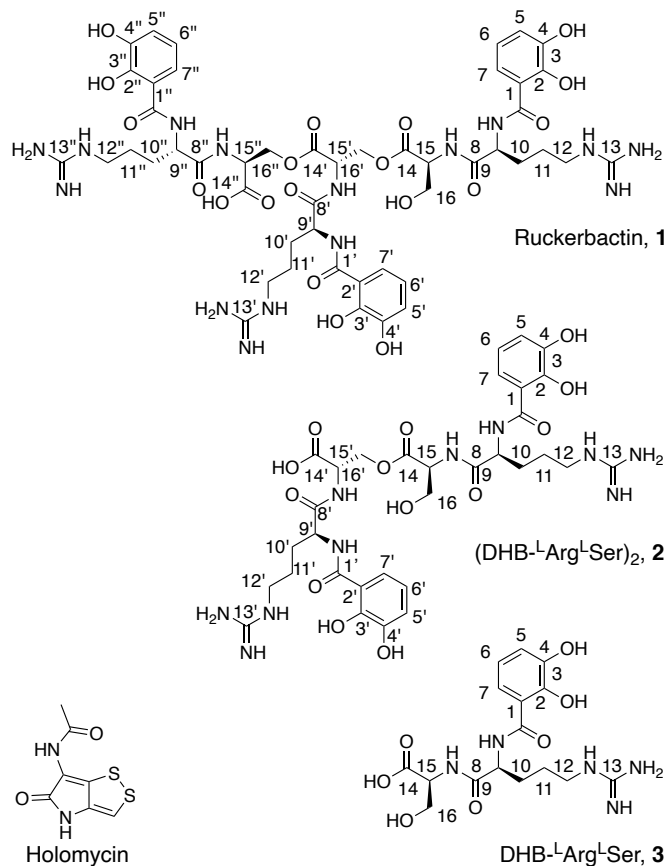


Figure 2. ESI MSMS of ruckerbactin (**1**).



The structures of ruckerbactin and the related biscatechol **2** and monocatechol **3** compounds were evaluated by NMR spectroscopy (Figures S6-S27 and Tables S1-S3). Similar resonances were observed in the NMR spectra of all three compounds, although with greater complexity in the spectra of **1** and **2** compared to **3**. The NMR spectra of **3** are quite similar to those of vanchrobactin, as would be expected for diastereomeric compounds, and as we show below, the only difference is the chirality of Arg. A combination of Ser α and β protons and Arg α protons overlap in the ^1H spectrum of the biscatechol compound **2**, and more so for ruckerbactin, as is apparent in the expanded region in the ^1H spectrum of **1** (Figure S9). The overlapping peaks in the Ser residues in **1** and **2** were deconvoluted by first mapping out their chemical shifts using COSY and HSQC. The order of each asymmetric residues was subsequently determined from correlations in the HMBC spectrum between β protons in Ser and carbonyl carbons in the esters

(Figure 3). Having determined the shifts of the α protons in the Ser residues in ruckerbactin, the chemical shifts of their amide protons were determined via COSY (Figure S10 and S11).

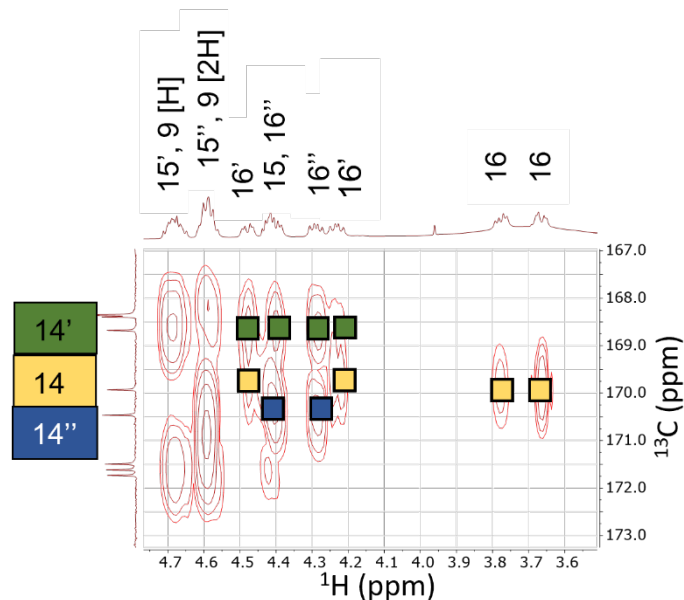


Figure 3. Expanded region of the ^1H - ^{13}C HMBC spectrum in the vicinity of the Ser residues of ruckerbactin (**1**).

Chiral amino acid analysis reveals the difference between ruckerbactin and trivanchrobactin (**6**). Ruckerbactin and compounds **2** and **3** were acid hydrolyzed and subsequently derivatized with Marfey's reagent (1-fluoro-2-4-dinitrophenyl-5-L-alanine amide, FDAA).¹³ HPLC separation of the FDAA-derivatized amino acids in the presence of added FDAA-derivatized standards of $^{\text{L}}$ Arg, $^{\text{D}}$ Arg, $^{\text{L}}$ Ser and $^{\text{D}}$ Ser established the presence of $^{\text{L}}$ Arg and $^{\text{L}}$ Ser in **1-3** (Figure S28). Thus, the chiral amino acid analysis confirmed the genomic prediction of $^{\text{L}}$ Ser and $^{\text{L}}$ Arg in ruckerbactin, $(\text{DHB}^{\text{L}}\text{Arg}^{\text{L}}\text{Ser})_3$, making it the diastereomeric counter to trivanchrobactin, $(\text{DHB}^{\text{D}}\text{Arg}^{\text{L}}\text{Ser})_3$.

The question arises whether $^{\text{L}}$ Arg in ruckerbactin sets the chirality at the Fe(III) site in Fe(III)-ruckerbactin in the same manner that $^{\text{L}}$ Lys directs formation of the Δ configuration in Fe(III)-

frederiksénibactin.³ In an octahedral metal complex, tris bidentate catechol coordination may result in either the Δ or Λ configuration (not taking into account the meridional and facial geometries imposed by the asymmetry of 2,3-DHBA). Enterobactin (**5**), the macrolactone of $(\text{DHB}^{\text{L}}\text{Ser})_3$, and its synthetic enantiomer, the macrolactone of $(\text{DHB}^{\text{D}}\text{Ser})_3$ adopt the Δ and Λ configurations, respectively, on coordination of Fe(III),^{14,15} demonstrating the influence of D- and L-Ser on the chirality of the Fe(III) complex. Electronic circular dichroism (ECD) spectroscopy was therefore employed to investigate the influence of ^LArg versus ^DArg on the chirality of Fe(III)-ruckerbactin in comparison to Fe(III)-trivanchrobactin. The ECD spectra of Fe(III)-ruckerbactin and Fe(III)-trivanchrobactin display four bands which are inverted in sign and intensity from each other (Figure 4; Table S4). Ligand to metal charge transfer (LMCT) gives rise to transitions in the region of 380 nm to 660 nm (Figure 4). The 295-380 nm region is dominated by ligand centered $\pi \rightarrow \pi^*$.¹⁴ Fe(III)-ruckerbactin follows the same pattern in the LMCT region of the spectrum as Fe(III)-enterobactin which is known to adopt the Δ configuration.^{14,15} The absolute configuration at the Fe(III) coordination center in Fe(III)-ruckerbactin is therefore Δ . Fe(III)-trivanchrobactin, on the other hand, forms the Λ configuration, as is evident from the inverted ECD signal.

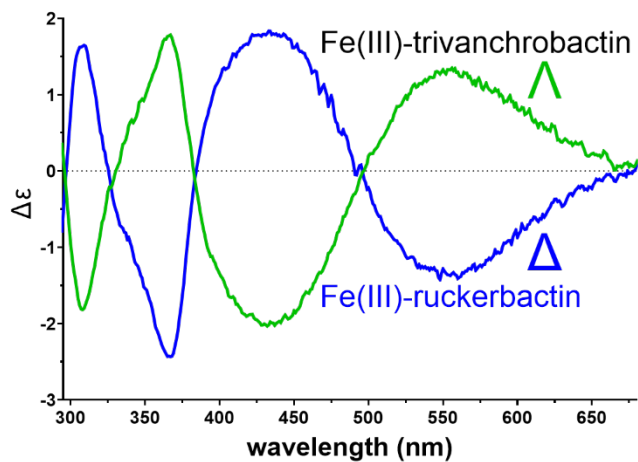


Figure 4. ECD spectra of Fe(III)-ruckerbactin and Fe(III)-trivanchrobactin. Conditions: 111 μ M Fe(III)-ruckerbactin (93 mM Bis-tris, pH 7) and 103 μ M Fe(III)-trivanchrobactin (89 mM Bis-tris, pH 7).

The antimicrobial and cytotoxic natural product holomycin (**4**),¹⁶ produced by *Y. ruckeri* ATCC 29473,¹⁷ was also isolated from the culture supernatant of *Y. ruckeri* YRB. Holomycin was identified by NMR, HRESI-MS and UV-Vis spectroscopy in comparison to previously reported spectra (Table S5, Figure S2).^{17, 18} The UV-Vis spectrum displays the same peaks and relative intensities as those reported for oxidized holomycin (Figure S1).¹⁸ Analysis of the *Y. ruckeri* YRB genome with antiSMASH¹⁹ revealed a putative holomycin BGC (BD65_566 – BD65_582) which is nearly identical to the holomycin locus of *Y. ruckeri* ATCC 29473 (97% nucleotide identity).¹⁷ A link between the potency of holomycin and siderophore-mediated iron uptake was previously reported in *E. coli*.²⁰ The bioactive state of holomycin is its reduced form, wherein the dithiol coordinates Zn(II) and other transition metal ions; thus reduced holomycin disrupts intracellular metal ion homeostasis.

In conclusion, we have structurally characterized the previously predicted catechol siderophore, ruckerbactin,⁹ as the linear oligoester (DHB^LArg^LSer)₃, along with the biscatechol **2**, (DHB^LArg^LSer)₂, and monocatechol **3**, DHB^LArg^LSer compounds. Ruckerbactin presents as the diastereomer to trivanchrobactin, (DHB^DArg^LSer)₃, produced by the marine bacterium *Vibrio campbellii* DS40M4,¹ which is also a fish pathogen along with *Y. ruckeri* YRB. Circular dichroism spectroscopy reveals the chirality of ^LArg and ^DArg amino acids appended to 2,3-DHB sets the enantiomeric configuration at the Fe(III) center, with Fe(III)-ruckerbactin adopting the Δ configuration and Fe(III) trivanchrobactin adopting the Λ configuration.

Recently the tris catechol siderophore, frederiksenibactin was reported from *Yersinia frederiksenii* ATCC 3364, which is the oligoserine (DHB^LLys^LSer)₃. Fe(III)-frederiksenibactin, like Fe(III)-ruckerbactin, adopts the Δ configuration at the Fe(III) site,³ as a result of the presence of ^LLys. While the true diastereomer of frederiksenibactin is not known, the macrolactone of (DHB^DLys^LSer)₃ is the siderophore cyclic trichrysobactin (CTC) produced by the plant pathogen *Dickeya chrysanthemi* EC16.^{2, 3} The BGCs for frederiksenibactin in *Y. frederiksenii* ATCC 3364 and CTC in *D. chrysanthemi* EC16 are also consistent with the presence of ^LLys and ^DLys, respectively, with the presence of an epimerase in the BGC in *D. chrysanthemi* EC16.³ Moreover the chirality at the Fe(III) site for Fe(III)-frederiksenibactin, Δ , and Fe(III)-CTC, Λ , matches the chirality of Fe(III) coordination by ruckerbactin, Δ , and trivanchrobactin, Λ . Further investigations into the effect of chirality at the Fe(III)-site of ruckerbactin and trivanchrobactin on iron uptake and utilization is in progress. Initial investigations with other enantiomeric Fe(III)-siderophores hint at the general importance of chirality to bacterial iron uptake processes.^{14, 21, 22}

Experimental Section

General Experimental Procedures. UV-Vis spectra were obtained on a Agilent CARY-300 spectrophotometer. ECD spectra were recorded on a Jasco J-1500 Circular dichroism spectropolarimeter. NMR spectroscopy was performed on a Bruker Avance NEO, 500 MHz with a prodigy BBO cryo probe. The solvent peak of DMSO-*d*₆ was used to reference the ¹H (δ 2.50) and ¹³C (δ 39.52) shifts. HRESI-MS was carried out on a Waters/ Micromass LCT Premier (UC Irvine) with isocratic MeOH flow at 0.2 mL/min and 10 μ L injection volume. ESI-MS/MS was performed on a Waters Xevo G2-XS QToF with positive mode electrospray ionization coupled to an ACQUITY UPLC H-Class system with a Waters BEH C18 column. Analytical

HPLC separations, including chiral amino acid analysis, was performed using a YMC AQ12S05-2546WT reverse phase (RP) column and two Waters 515 HPLC pumps. The eluents were a) doubly deionized H₂O (dd-H₂O) from an EMD Milli Pore IQ 7000 purification system 18 MΩ and b) HPLC-grade MeCN with 0.05% w/v trifluoroacetic acid (TFA). An MeCN gradient of 0.5%/min from 5-25% and a flowrate of 1 mL/min was used to analyze the crude extract. For isolation of the siderophores, semi-preparative HPLC was performed using a YMC AQ12S05-2520WT column in conjunction with two Waters 515 HPLC pumps. The compounds in the crude extract were separated using a 15-60% MeOH gradient, 7 mL per min, 1.8% per min. Both the aqueous and methanolic eluents were amended with 0.05% w/v TFA. For the second and final purification of compound **3**, a 15-25%, 0.5%/min. Compound **7** and ruckerbactin (**1**) were isolated using 25-35% gradient, 0.5%/min, 7 mL per min. All glassware was acid washed with 2 M HCl. Trivanchrobactin was obtained by hydrolysis of the macrolactone of (DHB^DArg^LSer)₃ which was synthesized as previously reported for the analogous Lys compounds.³

Bacterial Growth for Siderophore Isolation. Iron-deficient media for bacterial growth consisted of 10.0 g NaCl, 4.0 g NH₄Cl, 12.0 g Na₂HPO₄ • 7H₂O, 6.0 g KH₂PO₄, 6.0g MgSO₄ • 7H₂O and 100 mg CaCl₂ • 2H₂O dissolved in 1.9 L dd-H₂O with the pH adjusted to 7.4. After autoclaving the media, 100 mL of filter-sterilized anhydrous D-glucose, 6g/100 mL was added. *Y. ruckeri* YRB was cultured in 2 L media in 4 L Erlenmeyer flasks on an orbital shaker at 180 RPM. Each culture was inoculated with 4 mL of a starter culture of the same medium, and grown at RT. Once the cultures reached stationary phase of growth (OD₆₀₀ of 1.5), they were pelleted by centrifugation (Sorvall Evolution RC) equipped with an SLA-3000 rotor at 6000 RPM for 30 min at 4 °C. Amberlite® XAD-4 was added to the supernatant. This solution was incubated on a shaker, 140 RPM for 4 hours at room temperature or in the fridge overnight. The resin was

rinsed with 500 mL dd-H₂O prior to transferring it to a gravity chromatography column where 500 mL MeOH (HPLC grade), was used to elute metabolites. The eluent was subsequently concentrated by rotary evaporation at 40 °C and the metabolites separated by semi-preparative HPLC. The purified compounds were flash frozen and lyophilized for further characterization. A total of seven 2 L cultures yielded 14.0 mg ruckerbactin (**1**), 13.1 mg of compound **2** and 5.9 mg of compound and 4.46 mg compound **4**. NMR was run on these compounds dissolved in DMSO-*d*₆ from Cambridge Isotope Laboratories, Inc. 99.9%.

Ruckerbactin (1): light grey powder; UV-Vis, λ_{max} (log ϵ) 331 nm (4.055), ¹H, ¹³C, and 2D NMR data, Table S1, HRESIMS *m/z* 1156.4657 [M + H]⁺ (calcd for C₄₈H₆₆N₁₅O₁₉, 1156.4659).

Biscatechol Compound 2: ¹H, ¹³C, and 2D NMR data, Table S2, HRESIMS *m/z* 777.3178 [M + H]⁺ (calcd for C₃₂H₄₅N₁₀O₁₃, 777.3138).

Monocatechol Compound 3: ¹H, ¹³C, and 2D NMR data, Table S3, HRESIMS *m/z* 398.1678 [M + H]⁺ (calcd for C₁₆H₂₄N₅O₇, 398.1676).

Holomycin (4): yellow powder, ¹H, ¹³C, and 2D NMR data, Table S5, HRESIMS *m/z* 236.9769 [M + Na]⁺ (calcd for C₇H₆N₂O₂S₂Na, 236.9768).

Chiral amino acid analysis. For chiral amino acid analysis, compounds **1-3** were hydrolyzed in 1 M HCl acid under conditions of 400 μ L of a 1 mg/mL siderophore solution sealed in a glass ampule, and placed in an oven 110 °C for 19.5 h. Subsequently the hydrolyzed samples were transferred to a heating block 80 °C, resuspended in 1-2 mL dd-H₂O and subjected to three cycles of drying and resuspension in H₂O. The final dry hydrolysis products were resuspended in 100 μ L dd-H₂O. Amino acid standards were prepared by separately dissolving D-serine (\geq 98%), L-serine (99%), D-arginine hydrochloride (99%) and L-arginine hydrochloride (\geq 98%) in dd-H₂O at 1 mg/mL. The hydrolyzed siderophore samples and amino acid standards were derivatized by

Marfey's reagent (1-fluoro-2-4-dinitrophenyl-5- L-alanine amide, FDAA) by aliquoting 100 μ L of sample addition of 200 μ L of 6.8 mM Marfey's reagent (dissolved in acetone) and 40 μ L 10 mM sodium bicarbonate. The samples were incubated at 40 °C for 1 h, after which the reaction was quenched by addition of 20 μ L of 2 M HCl. The injections of the derivatized siderophores were prepared by diluting 40 μ L derivatized sample by addition of 60 μ L 1:1 acetone:H₂O. Co-injections with derivatized D- or L-Ser standards were prepared by mixing 40 μ L siderophore sample, 20 μ L FDAA-^D or ^LSer standard and 40 μ L 50% acetone and 50% H₂O. Co-injections with derivatized D- or L-Arg were prepared by mixing 40 μ L siderophore sample and 60 μ L FDAA-^D or ^LArg standard. Analytical HPLC was run by injecting 50 μ L of the spiked samples. The eluents were a) 50 mM triethylamine (99%) and sodium phosphate monobasic (99.9%) in dd-H₂O with pH adjusted to 3.0 and b) MeCN. For compounds **2** and **3**, the analytical HPLC method was 10-50% MeCN with a gradient of 0.667% per min and a flowrate of 1 mL/min and for ruckerbactin 20-35% MeCN, 0.33% per min and a flowrate of 1 mL/min.

Ruckerbactin titration with Fe(III). Apo ruckerbactin was titrated spectrophotometrically (Agilent CARY-300) with a stock solution of 2.69 mM \pm 0.03 Fe(III) (FeCl₃ • 6 H₂O) in 25 mM HCl. The stock was standardized spectrophotometrically with 1,10 phenanthroline (510 nm, ϵ 1.1 \times 10⁴ M⁻¹cm⁻¹). The break point at 1:1 Fe(III):ruckerbactin yields an extinction coefficient for Fe(III)-ruckerbactin, $\epsilon_{498\text{ nm}}$, of 4,709 M⁻¹cm⁻¹ (Figure S29). By comparison, titration of apo trivanchrobactin with Fe(III) yields an extinction coefficient of Fe(III)- trivanchrobactin, ϵ_{498} , of 4,969 M⁻¹cm⁻¹ (Figure S29). Based on the 1:1 coordination of Fe(III)-the tris catechol siderophores, extinction coefficients for apo-ruckerbactin, $\epsilon_{331\text{nm}}$ 11,353 M⁻¹cm⁻¹ and apo-trivanchrobactin, ϵ_{330} 10,612 M⁻¹cm⁻¹ were also calculated.

Electronic Circular Dichroism (ECD) Spectroscopy of Fe(III)-Siderophore Complexes. The absolute configuration of Fe(III)-ruckerbactin and Fe(III)-trivanchrobactin were evaluated by ECD spectroscopy under conditions of 111 μ M Fe(III)-ruckerbactin in 93 mM Bis-tris, pH 7.0 and 103 μ M Fe(III)-trivanchrobactin in 89 mM Bis-tris, pH 7, using an enantiomeric reference of equimolar (48 μ M) Fe(III)-(DHB^DLys-^DSer)₃ and Fe(III)-(DHB^LLys-^LSer)₃ in 92 mM Bis-Tris buffer, pH 7.0.^{3 23} The ECD spectra (Jasco J-1500 CD spectropolarimeter) were recorded using the following settings: 1 nm data pitch, bandwidth 1 nm, 20 mdeg digital scale, DIT 8 sec. and a 20 nm/min scan speed, between 800-230 nm with 3 accumulations of each sample. All measurements were carried out in the same 1 cm quartz cuvette in the same orientation. The UV-Vis spectra of the Fe(III)-ruckerbactin and Fe(III)-trivanchrobactin samples used for ECD spectroscopy are in Figure S30.

ASSOCIATED CONTENT

Supporting Information. The Supporting Information is available free of charge at <https://publs.acs.org/doi>

MS, chiral amino acid analyses, 1D and 2D ¹H and ¹³C NMR of ruckerbactin and compounds **2-4**, UV-Vis and Fe(III)-titrations of ruckerbactin, and BGC analysis of holomycin.

AUTHOR INFORMATION

Corresponding Author

* Alison Butler – Department of Chemistry & Biochemistry, University of California, Santa Barbara, CA 93106-9510 United States; orcid.org/0000-0002-3525-7864; email: butler@chem.ucsb.edu

Authors

Emil Thomsen – Department of Chemistry & Biochemistry, University of California, Santa Barbara, CA 93106-9510 United States; orcid.org/0000-0002-0451-2121

Zachary L. Reitz – Department of Chemistry & Biochemistry, University of California, Santa Barbara, CA 93106-9510 United States; orcid.org/0000-0003-1964-8221

Parker Stow – Department of Chemistry & Biochemistry, University of California, Santa Barbara, CA 93106-9510 United States; orcid.org/0000-0002-1238-0616

Kalana Dulaney – Department of Chemistry & Biochemistry, University of California, Santa Barbara, CA 93106-9510 United States

Author Contributions

All authors contributed to the experiments reported in this manuscript. All authors have given approval to the final version of the manuscript.

Acknowledgement

Funding from NSF CHE-1710761 (A.B.) and a UC Regents Graduate Fellowship (E.T.) is gratefully acknowledged.

References

1. Sandy, M.; Han, A.; Blunt, J.; Munro, M.; Haygood, M.; Butler, A., Vanchrobactin and anguibactin siderophores produced by *Vibrio* sp. DS40M4. *J. Nat. Prod.* **2010**, *73* (6), 1038-1043.
2. Sandy, M.; Butler, A., Chrysobactin siderophores produced by *Dickeya chrysanthemi* EC16. *J. Nat. Prod.* **2011**, *74* (5), 1207-1212.
3. Stow, P. R.; Reitz, Z. L.; Johnstone, T. C.; Butler, A., Genomics-driven discovery of chiral trisicatechol siderophores with enantiomeric Fe(iii) coordination. *Chem Sci* **2021**, *12*, 12485-12493.
4. Wilson, M. K.; Abergel, R. J.; Raymond, K. N.; Arceneaux, J. E. L.; Byers, B. R., Siderophores of *Bacillus anthracis*, *Bacillus cereus*, and *Bacillus thuringiensis*. *Biochem Bioph Res Co* **2006**, *348* (1), 320-325.
5. Han, A. W.; Sandy, M.; Fishman, B.; Trindade-Silva, A. E.; Soares, C. A. G.; Distel, D. L.; Butler, A.; Haygood, M. G., Turnerbactin, a novel trisicatecholate siderophore from the shipworm endosymbiont *Teredinibacter turnerae* T7901. *PLoS One* **2013**, *8* (10), e76151.
6. Budzikiewicz, H.; Bossenkamp, A.; Taraz, K.; Pandey, A.; Meyer, J. M., Bacterial constituents#72. Corynebactin, a cyclic catecholate siderophore from *Corynebacterium glutamicum* ATCC 14067 (*Brevibacterium* sp. DSM 20411). *Z Naturforsch C* **1997**, *52* (7-8), 551-554.
7. Matsuo, Y.; Kanoh, K.; Jang, J. H.; Adachi, K.; Matsuda, S.; Miki, O.; Kato, T.; Shizuri, Y., Streptobactin, a Tricatechol-Type Siderophore from Marine-Derived *Streptomyces* sp YM5-799. *J Nat Prod* **2011**, *74* (11), 2371-2376.
8. Romalde, J. L.; Toranzo, A. E., Pathological Activities of *Yersinia ruckeri*, the Enteric Redmouth (Erm) Bacterium. *Fems Microbiol Lett* **1993**, *112* (3), 291-300.
9. Fernandez, L.; Marquez, I.; Guijarro, J. A., Identification of specific in vivo-induced (ivi) genes in *Yersinia ruckeri* and analysis of ruckerbactin, a catecholate siderophore iron acquisition system. *Appl Environ Microb* **2004**, *70* (9), 5199-5207.
10. Romalde, J. L.; Conchas, R. F.; Toranzo, A. E., Evidence That *Yersinia ruckeri* Possesses a High-Affinity Iron Uptake System. *Fems Microbiol Lett* **1991**, *80* (2-3), 121-126.
11. Kumar, G.; Hummel, K.; Ahrens, M.; Menanteau-Ledouble, S.; Welch, T. J.; Eisenacher, M.; Razzazi-Fazeli, E.; El-Matbouli, M., Shotgun proteomic analysis of *Yersinia ruckeri* strains under normal and iron-limited conditions. *Vet Res* **2016**, *47*.
12. Shek, P. Y. I.; Zhao, J.; Ke, Y.; Siu, K. W. M.; Hopkinson, A. C., Fragmentations of protonated arginine, lysine and their methylated derivatives: Concomitant losses of carbon monoxide or carbon dioxide and an amine. *J Phys Chem A* **2006**, *110* (27), 8282-8296.
13. Marfey, P., Determination of D-Amino Acids .2. Use of a Bifunctional Reagent, 1,5-Difluoro-2,4-Dinitrobenzene. *Carlsberg Res Commun* **1984**, *49* (6), 591-596.
14. Abergel, R. J.; Zawadzka, A. M.; Hoette, T. M.; Raymond, K. N., Enzymatic Hydrolysis of Trilactone Siderophores: Where Chiral Recognition Occurs in Enterobactin and Bacillibactin Iron Transport. *J Am Chem Soc* **2009**, *131* (35), 12682-12692.
15. Johnstone, T. C.; Nolan, E. M., Determination of the Molecular Structures of Ferric Enterobactin and Ferric Enantioenterobactin Using Racemic Crystallography. *J Am Chem Soc* **2017**, *139* (42), 15245-15250.

16. Ding, H.; Wang, J. N.; Zhang, D. S.; Ma, Z. J., Derivatives of Holomycin and Cyclopropaneacetic Acid from *Streptomyces* sp DT-A37. *Chem Biodivers* **2017**, *14* (9), e1700140.

17. Qin, Z. W.; Baker, A. T.; Raab, A.; Huang, S.; Wang, T. H.; Yu, Y.; Jaspars, M.; Secombes, C. J.; Deng, H., The Fish Pathogen *Yersinia ruckeri* Produces Holomycin and Uses an RNA Methyltransferase for Self-resistance. *J Biol Chem* **2013**, *288* (21), 14688-14697.

18. Yin, H.; Xiang, S. H.; Zheng, J. T.; Fan, K. Q.; Yu, T. T.; Yang, X.; Peng, Y. F.; Wang, H. B.; Feng, D. Q.; Luo, Y. M.; Bai, H.; Yang, K. Q., Induction of Holomycin Production and Complex Metabolic Changes by the *argR* Mutation in *Streptomyces clavuligerus* NP1. *Appl Environ Microb* **2012**, *78* (9), 3431-3441.

19. Blin, K.; Shaw, S.; Kloosterman, A. M.; Charlop-Powers, Z.; van Wezel, G. P.; Medema, Marnix H.; Weber, T., antiSMASH 6.0: improving cluster detection and comparison capabilities. *Nucleic Acids Research* **2021**, *49* (W1), W29-W35.

20. Chan, A. N.; Shiver, A. L.; Wever, W. J.; Razvi, S. Z. A.; Traxler, M. F.; Li, B., Role for dithioliopyrrolones in disrupting bacterial metal homeostasis. *P Natl Acad Sci USA* **2017**, *114* (10), 2717-2722.

21. Youard, Z. A.; Wenner, N.; Reimann, C., Iron acquisition with the natural siderophore enantiomers pyochelin and enantio-pyochelin in *Pseudomonas* species. *Biometals* **2011**, *24* (3), 513-522.

22. Winkelmann, G.; Braun, V., Stereoselective Recognition of Ferrichrome by Fungi and Bacteria. *Fems Microbiol Lett* **1981**, *11* (4), 237-241.

23. Malon, P.; Keiderling, T. A., A Solution to the Artifact Problem in Fourier-Transform Vibrational Circular-Dichroism. *Appl Spectrosc* **1988**, *42* (1), 32-38.

TOC Graphic

